Characterization of Adducts Formed in the Reactions of Methylglyoxal and Malonaldehyde with Lysine and Histidine Derivatives

by **Donata Pluskota-Karwatka*** and **Agata Pawłowska**

Adam Mickiewicz University in Poznań, Faculty of Chemistry, Umultowska 89b, PL-61-614 Poznań (phone: +48-61-8291692; e-mail: donatap@amu.edu.pl)

Glycation of biopolymers by α-oxoaldehydes such as methylglyoxal is believed to play a major role in the complex pathologies associated with diabetes and metabolic diseases. To design strategies that could interfere with the endogenous production of such aldehydes or promote their detoxification or, alternatively, to develop therapeutic procedures that could inhibit the deleterious effects of the oxoaldehydes at the cellular level, it is important to characterize the wide spectrum of reactions between these compounds and biomolecules, and gain insight into their mechanisms. In this study, we investigated the reactivity of endogenous α-oxoaldehyde, methylglyoxal, and of malonaldehyde towards amino acid derivatives, and we identified new adducts with N^{α}-acetyllysine and N^{α}-acetylhistidine. In addition, we showed that a structurally analogous adduct is also formed with the model peptide *N*-acetylglycyllysine *O*-methyl ester. The characterized compounds were most likely derived from the addition of the appropriate nucleophilic center of the studied biomolecules to the C=C bond of the initially formed aldehyde conjugate. The resulted adducts contain an electrophilic β-dicarbonyl moiety and could potentially be involved in the formation of DNA–protein or protein cross–links.

1. Introduction. – α-Dicarbonyl compounds represent environmental contaminants, but are also natural products formed during a number of cellular processes. One of the most prominent α-oxoaldehydes is methylglyoxal, a highly reactive metabolite derived from several nonenzymatic and enzymatic reactions. Degradation of triosephosphates, lipid peroxidation, side reactions from glucose-mediated glycation, and deamination of aminoacetone are major processes associated with the formation of methylglyoxal *in vivo* [1–3]. Methylglyoxal has been identified as a precursor of advanced glycation end products (AGEs) which comprise a structurally diverse class of lipid, DNA [4], and protein [5] modifications formed in living organisms. Protein AGEs are believed to be involved in the pathologies associated with aging, cancer, and *Alzheimer*'s disease, as well as with diabetes-related complications, including nephropathy, vascular impairment, and immune suppression [6][7]. Methylglyoxal can irreversibly modify amino acid residues of proteins such as bovine serum albumin, collagen, ribonuclease A, and cytosolic aspartate aminotransferase leading to alteration of their normal function [8][9]. It has been reported that methylglyoxal reacts with arginine to form 5-methylimidazolone, 5-hydro-5-methylimidazolone, and argpyrimidine [10][11], and also with lysine to generate imidazolysine and N^{ε}-carboxyethyllysine [12], which accumulate with aging and its related diseases. Apart from methylglyoxal, a range of other aldehydes can be produced in biological systems. These continuously formed electrophiles can coexist in biological tissues and can modify biopolymers in a synergistic manner [13]. The resulted adducts may represent more harmful lesions than

those generated by individual mutagenic agents. It has been shown that malonaldehyde and acetaldehyde react simultaneously with proteins forming adducts that comprise units derived from both aldehydes [13]. The same protein modifications have been identified in EtOH-fed rats and in patients with alcohol-induced liver disease [14].

Recently, we identified methylglyoxal adducts of adenine nucleosides generated in the presence of malonaldehyde [15], and we demonstrated that in model reactions with N^{α}- and N^{ε}-acetyllysine these adducts are capable of inducing a new class of DNA-protein cross-links [16]. In the present study, we investigated the reactivity of methylglyoxal and malonaldehyde towards amino acids, and we characterized new adducts of N^{α}-acetyllysine and N^{α}-acetylhistidine. In addition, we showed that the analogous adduct is also formed with the model dipeptide *N*-acetylglycyllysine *O*-methyl ester. Lysine and histidine are, besides cysteine and arginine, major targets for electrophilic compounds [17–22]. These amino acids are also very often involved in the formation of protein AGEs containing both cross-linking and non-cross-linking adducts. Despite their ubiquitous formation in living cells and their biological significance, still little is known and much remains to be learned about the structural features and mechanisms of the formation of these types of lesions. Structural characterization of the wide spectrum of adducts generated between electrophilic products of cellular processes and biomolecules *in vitro* may provide insight into the chemical nature of modifications possibly formed in living organisms. Although findings derived from studies with model systems may not always be pertinent to more complicated biological systems, they can be of help in clarifying mechanisms involved in acting of endogenously formed deleterious chemicals such as α-oxoaldehydes.

2. Results and Discussion. – In this work, we studied the reactivity of methylglyoxal and malonaldehyde towards N^{α}-acetyllysine, N^{α}-acetylhistidine, and *N*-acetylglycyllysine *O*-methyl ester, respectively, so the electrophiles could only interact with N^{ε} of the lysine derivatives and N^{π} or/and N^{τ} of the histidine imidazole ring.

2.1. *Reaction of Methylglyoxal and Malonaldehyde with* N^{α}*-Acetyllysine.* Methylglyoxal and malonaldehyde were subjected to a reaction with N^{α}-acetyllysine in an aqueous phosphate buffer solution at pH 4.6, at 37° for 2 d. LC Analysis of the mixture revealed that the aldehydes gave rise to one adduct (*Scheme 1*, M_1MG-ALys; **1**). The UV spectrum of this product exhibited an absorption maximum at 265 nm. In the ESI-MS, the $[M+1]^+$ signal of the adduct was observed at *m*/*z* 315. In the MS^2 measurement of *m*/*z* 315, the signal at *m*/*z* 189 corresponded to the cleavage of the malonaldehyde-methylglyoxal unit from the modified amino acid, followed by the attachment of a H-atom. The adduct was stable during the isolation and purification steps. ^{1}H- and ^{13}C-NMR chemical shifts, ^{1}H,^{1}H-coupling constants, and HMBC in the NMR spectra of M_1MG-ALys (**1**) are summarized in *Table 1*.

The ^{1}H-NMR spectrum of the compound displayed three signals, besides the signals of H-atoms from the N^{α}-acetyllysine moiety. The signal at 8.80 ppm was assigned to the two chemically equivalent aldehyde H-atoms on the basis of the chemical shift and the HSQC with the C-signal at 192.8 ppm. The 1 H *singlet* that appeared at 4.85 ppm was assigned to H–C(b) on the basis of the one-bond ^{1}H,^{13}C-correlation with the C-signal at 62.9 ppm, and further based on HMBCs between this H-signal and signals attributed to

Table 1. *^{1}H-, ^{13}C-NMR Data, and Long-Range HMBCs of M_1MG-ALys* (**1**). δ in ppm, J in Hz.

	δ(H)		δ(C)	HMBC
CHO	8.80 (*s*)	CHO	192.8	H–C(b)
H–C(b)	4.85 (*s*)	C(b)	62.9	C*H*O, H_a–C(ε), *Me*(C=O)–C(b)
H–C(a)	no[a])	C(a)	112.1	H–C(b)
Ac–C(b)	2.14 (*s*)	Ac–C(b)	208.6	*Me*(C=O)–C(b), H–C(b)
		Ac–C(b)	27.8	
H–C(α)	4.12 (*dd*, J = 8.0, 4.6)	C(α)	57.6	Me(acetyllysine), H_a–C(β), H_b–C(β), H–C(γ)
CH_2(ε)	2.98 – 2.93 (*m*, H_a), 2.92 – 2.87 (*m*, H_b)	C(ε)	47.5	H–C(b)
CH_2(δ)	1.69 – 1.65 (*m*)	C(δ)	27.9	H_a–C(ε), H_b–C(ε), H–C(γ)
CH_2(β)	1.82 – 1.76 (*m*, H_a), 1.69 – 1.65 (*m*, H_b)	C(β)	33.9	H–C(α), H–C(γ)
CH_2(γ)	1.39 – 1.34 (*m*)	C(γ)	25.2	H_a–C(ε)
Me (acetyllysine)	2.02 (*s*)	Me	24.7	
		Me(*C*=O) (acetyllysine)	176.5	Me (acetyllysine), H–C(α)
		*C*OOH	182.0	H–C(α), H_a–C(β), H_b–C(β)

[a]) Not observed, due to the acidity of the H-atom.

the C(ε), CHO, Me(*C*=O)–C(b), and C(a). The Me signal at 2.14 ppm was assigned to the Me group derived from methylglyoxal on the basis of the chemical shift and the one-bond ^{1}H,^{13}C-correlation with the C-signal at 27.8 ppm. In the ^{13}C-NMR spectrum, five signals were observed in addition to the signals arising from the amino acid unit. The signals observed at 192.8, 62.9, and 27.8 ppm were assigned to the *C*HO, C(b), and *Me*(C=O)–C(b) atoms, respectively. The assignment of the signal at 208.6 ppm to Me(*C*=O)–C(b) atom was based on the chemical shift and strong correlation (HMBC) between this signal and the signal derived from the Me group (*Me*(C=O)–C(b)). The signal at 112.1 ppm was attributed to the C(a) atom. This atom is included in the structural fragment of the adduct that is derived from malonaldehyde. A very similar chemical shift (112.3 ppm) for the corresponding C-atom (labelled as C(2)), was observed in the ^{13}C-NMR spectrum of the malonaldehyde sodium salt [23]. The data collected from mass spectrometry and from NMR spectroscopy were consistent with the structure for M_1MG-ALys (**1**) as depicted in *Scheme 1*.

2.2. *Reaction of Methylglyoxal and Malonaldehyde with* N-*Acetylglycyllysine* O-*Methyl Ester.* LC Analysis of the mixture of methylglyoxal and malonaldehyde during the reaction with the model dipeptide showed the formation of one distinct product. The UV spectrum of this compound (M_1MG-Dipep (**2**), *Scheme 1*) displayed an absorption maximum at 265 nm and was very similar to the UV spectrum of M_1MG-ALys (**1**). In the ESI-MS, M_1MG-Dipep (**2**) gave rise to an $[M+1]^+$ signal at m/z 386. In the MS^2 measurement of m/z 386, the signal at m/z 260 indicated the loss of the malonaldehyde-methylglyoxal unit. In the NMR spectra of compound **2**, the chemical shifts of the H- and C-atoms derived from the malonaldehyde-methylglyoxal core were very similar to those assigned for corresponding atoms in M_1MG-ALys (**1**; *Tables 2* and *1*, resp.).

Scheme 1. *Mechanism Proposed for the Formation of M_1MG-Alys* (**1**) *and M_1MG-Dipep* (**2**)

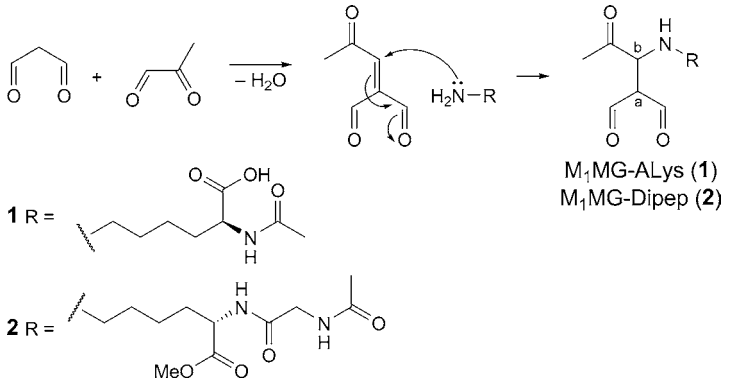

Table 2. *^{1}H-, ^{13}C-NMR Data, and Long-Range HMBCs of M_1MG-Dipep* (**2**). δ in ppm, J in Hz.

	δ(H)		δ(C)	HMBC
CHO	8.81 (*s*)	CHO	192.8	H–C(b)
H–C(b)	4.86 (*s*)	C(b)	62.9	CHO, H_a–C(ε), H_b–C(ε), Ac–C(b)
H–C(a)	no[a])	C(a)	112.1	H–C(b)
		Ac–C(b)	208.6	Ac–C(b), H–C(b)
Ac–C(b)	2.13 (*s*)	Ac–C(b)	27.4	
H–C(α)	4.43 (*ddd*, J = 9.2, 4.9, 2.8)	C(α)	55.1	H_a–C(β), H_b–C(β), H–C(γ)
MeO	3.75 (*s*)	MeO	55.7	
CH_2 (glycine)	3.92	CH_2 (glycine)	45.1	
CH_2(ε)	2.98 – 2.93 (*m*, H_a), 2.91 – 2.86 (*m*, H_b)	C(ε)	47.5	H–C(b), H–C(γ), H–C(δ)
CH_2(δ)	1.70 – 1.64 (*m*)	C(δ)	27.4	H_a–C(ε), H_b–C(ε), H–C(γ), H_a–C(β)
CH_2(β)	1.93 – 1.87 (*m*, H_a), 1.76 – 1.71 (*m*, H_b)	C(β)	32.4	H–C(α), H–C(γ,) H–C(δ)
CH_2(γ)	1.41 – 1.36 (*m*)	C(γ)	24.7	H–C(α), H_a–C(ε), H_b–C(ε), H–C(δ), H_b–C(β)
Me (acetylglycine)	2.05 (*s*)	Me	24.5	
		Me(*C*=O) (acetylglycine)	177.8	*Me* (acetylglycine), C*H*$_2$ (glycine)
		MeO(*C*=O)	177.1	*Me*O, H–C(α)
		CH_2(*C*=O)NH	174.6	C*H*$_2$ (glycine)

[a]) Not observed, due to the acidity of the H-atom.

This identity together with the MS and UV spectra of M_1MG-Dipep (**2**) strongly indicated that this compound was a structural analog of M_1MG-ALys (**1**).

2.3. *Reaction of Methylglyoxal and Malonaldehyde with* N$^{\alpha}$*-Acetylhistidine.* LC Analysis of the mixture of methylglyoxal and malonaldehyde with *N*$^{\alpha}$-acetylhistidine showed again formation of one product (*Scheme 2*). The UV spectrum of this compound displayed an absorption maximum at 268 nm. In the ESI-MS (positive-ion

Scheme 2. *Mechanism Proposed for the Formation of M_1MG-AHis-a* (**3a**)

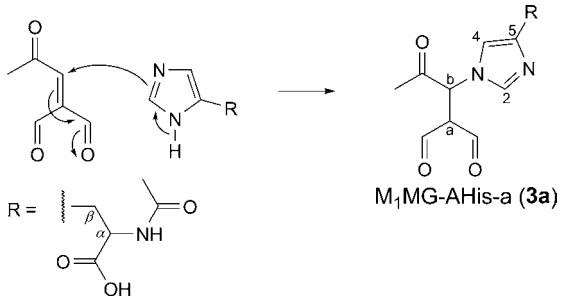

mode), this product showed an $[M+1]^+$ signal at *m/z* 324. In the MS^2 measurement of *m/z* 324, the signal observed at *m/z* 198 corresponded to the cleavage of the malonaldehyde-methylglyoxal unit. Isolation and purification of the adduct were carried out by using LC. NMR Analysis of the product revealed that it was a mixture of two isomers. The isolated product consisted of the N^τ (*Fig.*, M_1MG-AHis-a; **3a**) and N^π (*Fig.*, M_1MG-AHis-b; **3b**) regioisomers resulting in complex NMR spectra. In studies on the histidine adducts with styrene oxide, the N^τ derivatives predominated, indicating that the τ position of the imidazole ring is more reactive towards electrophilic agents [24]. In our studies, we also observed that one of the isomers was formed in a large excess. The NMR data sets for the signals arising from the N^α-acetylhistidine core of the predominated isomer M_1MG-AHis-a (**3a**; *Table 3*), were similar to those reported for other histidine modifications [24][25].

Apart from these signals, the ^{1}H-NMR spectrum of M_1MG-AHis-a (**3a**) displayed signals at 8.77, 3.64, and 2.17 ppm. The first signal, on the basis of a one-bond ^{1}H,^{13}C

Table 3. *^{1}H-, ^{13}C-NMR Data, and Long-Range HMBCs of M_1MG-AHis-a* (**3a**). δ in ppm, *J* in Hz.

	δ(H)		δ(C)	HMBC
CHO	8.77 (*s*)	CHO	192.6	
H–C(2)	7.78 (*s*)	C(2)	138.3	H–C(4), H_b–C(β)
H–C(4)	6.92 (*s*)	C(4)	120.5	H–C(2), H_a–C(β), H_b–C(β)
H–C(a)	no[a])	C(a)	111.4	H–C(b)
H–C(b)	3.64 (*s*)	C(b)	59.0	*Me*(C=O)–C(b), CHO
Ac–C(b)	2.17 (*s*)	Ac–C(b)	28.3	
H–C(α)	4.42 (*dd*, *J* = 8.6, 4.6)	C(α)	57.4	H_a–C(β), H_b–C(β), Me (Ac)
CH_2(β)	3.11 (*dd*, *J* = 15.0, 4.7, H_a), 2.96 (*dd*, *J* = 15.0, 8.7, H_b)	C(β)	31.7	H–C(α)
Me (Ac)	1.96 (*s*)	Me	24.7	
		(*C*=O)–C(b)	212.1	*Me*(C=O)–C(b)
		Me(*C*=O) (acetylhistidine)	176.3	Me (acetylhistidine), H–C(α)
		COOH	180.7	H–C(α), H_a–C(β), H_b–C(β)
		C(5)	135.5	H–C(2), H–C(4), H–C(α), H_a–C(β), H_b–C(β)

[a]) Not observed, due to the acidity of the H-atom.

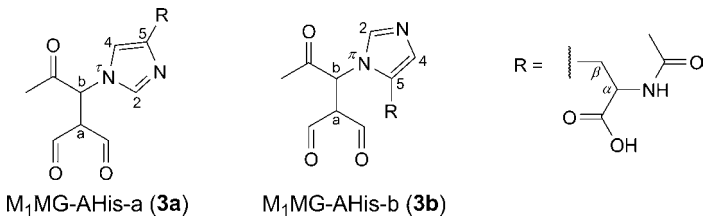

Figure. *Structures of the histidine adducts*

correlation (HSQC) with the C-atom signal at 192.6 ppm, was assigned to the aldehyde H-atoms. The signal at 3.64 ppm showed one-bond $^{1}H,^{13}C$-correlation with the C-atom signal at 59.0 ppm and was attributed to H–C(b), and the signal at 2.17 ppm was assigned to the *Me*(C=O)–C(b) group based on the chemical shift and a one-bond $^{1}H,^{13}C$-correlation with the C-atom signal at 28.3 ppm. The signal in the ^{13}C-NMR spectrum of compound M_1MG-AHis-a (**3a**) at 111.4 ppm was attributed to the C(a) atom, and the signal at 212.1 ppm to the C(b)(*C*=O) atom. These assignments were confirmed by strong correlations observed in the HMBC spectrum between the signal at 111.4 ppm and the signal attributed to H–C(b), and between the signal at 212.1 ppm and the signal assigned to the Me group (Ac–C(b)), respectively. The chemical shifts for H- and C-atoms in M_1MG-AHis-a (**3a**) that derived from the malonaldehyde-methylglyoxal unit were similar to those observed in M_1MG-ALys (**1**) and M_1MG-Dipep (**2**). This fact confirmed the structure depicted for M_1MG-AHis-a (**3a**) in the *Figure*.

^{1}H- and ^{13}C-chemical shifts of the minor isomer (M_1MG-AHis-b, **3b**; *Fig.*) were extracted from the spectra of the mixture of M_1MG-AHis-a (**3a**) and M_1MG-AHis-b (**3b**) as less intense signals and are presented in the *Exper. Part.*

2.4. *Mechanism for the Formation of the Malonaldehyde-Methylglyoxal Adducts of Amino Acids.* All isolated adducts contain units derived from the malonaldehyde-methylglyoxal conjugate. Previously, we identified the malonaldehyde-methylglyoxal adducts of adenine nucleosides, and we proposed that the mechanism responsible for these adducts formation implies 1,4-addition of the exocyclic amino group of the nucleobase to the initially formed conjugate of the studied aldehydes [15]. Earlier, we characterized a range of malonaldehyde-acetaldehyde adducts of DNA arising from interactions between the DNA bases and the malonaldehyde-acetaldehye condensation products [26]. The analogous mechanism is most likely responsible for the formation of the amino acid adducts characterized in this study. The compounds were proposed to be formed in the addition of the amino group of the lysine derivatives and one of the imidazole N-atoms of N^{α}-acetylhistidine, respectively, to the α,β-unsaturated dicarbonyl moiety of the malonaldehyde-methylglyoxal conjugate (*Schemes 1* and *2*).

3. Conclusions. – Modification of proteins and other biomolecules by electrophilic products of cellular processes is believed to play a significant role in the pathologies associated with free radical damage, including cardiovascular and neurological diseases, cancer, and aging [27]. Identification of the protein targets and elucidation of structures of the arising adducts are essential for clarifying mechanisms responsible

for the formation of such modifications. The model reactions examined in this study resulted in the structural characterization of previously unknown amino acid adducts formed by the interactions of lysine derivatives and N^{α}-acetylhistidine, respectively, simultaneously with methylglyoxal and malonaldehyde. The highest yield of these adducts were obtained under acidic conditions (pH 4.6), but their formation was also observed at physiological pH. These compounds may represent models for amino acid modifications by methylglyoxal and malonaldehyde. Lysine is an abundant amino acid in many proteins and is often located accessibly on their surfaces [28]. Despite the fact that lysine side chains are basic and extensively protonated at physiological pH, reactive electrophilic reagents are able to modify these chains under *in vivo* conditions [29][30]. Histidine is often situated more internally, but was also found to be a target for an attack of electrophiles [28]. Our studies confirmed that both amino acids can be involved in reactions with endogenously generated carbonyl compounds. Reactions with methylglyoxal and malonaldehyde can induce the formation of carbonyl groups in proteins and, as a consequence, can lead to initiation of the DNA-protein or protein cross-linking. Our results can provide a better understanding of the complex chemistry of the effects induced by dicarbonyl compounds of endogenous origin and can contribute to clarifying the role that α-oxoaldehydes play in the biochemistry of AGEs.

Experimental Part

General. Malonaldehyde was prepared by acidic hydrolysis of 1,1,3,3-tetramethoxypropane (TMP) as described by *Stone et al.* [31]. Methylglyoxal was purchased from *Fluka*. N^{α}-acetyllysine, TMP, NH_4HCO_3, and MeCN (gradient grade for chromatography) were purchased from *Sigma–Aldrich*. N^{α}-Acetylhistidine was purchased from *Trade Mark* and *N*-acetylglycyllysine methyl ester from *Bachem*.

Chromatographic Methods. Progress of the reactions was monitored by LC-DAD and the analyses were performed on an *Agilent 1100* series liquid chromatographic system consisting of a model *G1312A* binary pump, a *G1313A* autosampler, a *G1379A* vacuum degasser, a *G1315B* diode-array detector (UV), a 5 μm, 4.6 × 150 mm reversed-phase *C18* anal. column (*Hypersil Gold*, *Thermo Scientific*) and *Agilent ChemStation* data handling program (*Agilent Technologies*). The column was eluted isocratically for 5 min with 0.01M phosphate buffer, pH 7.1, and then with a gradient from 0% to 30% MeCN in 25 min at a flow rate of 1.5 ml/min.

Separation and purification of the adducts were carried out using a semiprep. 5 μm, 10 × 250 mm (*Hypersil Gold*, *Thermo Scientific*) reversed-phase *C18* column. The column was coupled to the *Agilent 1200* Series HPLC system consisting of a binary pump (*G1312A*), an autosampler (*G1329A*), a vacuum degasser (*G1379B*), a diode-array detector (UV; *G1315B*), a fraction collector (*G1364C*), and *Agilent ChemStation* data handling program (*Agilent Technologies*).

LC/ESI-MS Methods. The LC/ESI-MS analyses were performed with a *Waters ZQ* instrument equipped with an electrospray ion source and operated in both positive as well as negative-ion mode. Ionisation was carried out using N_2 as both nebulizer gas (80 l/min) and desolvation gas (300 l/h) heated to 300°. The capillary exit offset had a value of 3000 V and skim voltage was set to 30 V. The maximum ion accumulation time was 0.1 min. The analyzed adducts were introduced through the LC system using a reversed-phase *C18* analytical column (5 μm, 4.6 × 150 mm, *Symmetry*) eluted isocratically for 5 min with 1% MeCN in 0.01M $AcONH_4$, and then with a gradient from 1% to 30% MeCN during the course of 30 min at a flow rate of 0.5 ml/min.

NMR and UV Spectroscopy. The ^{1}H- and ^{13}C-NMR spectra of the adducts were recorded with a *Bruker UltraShield*™ *600* (*Bruker*, Germany) NMR spectrometer at 600 MHz in D_2O. The solvent was used as an internal reference standard. Two-dimentional NMR spectroscopy was used for structural evaluation of the compounds. ^{1}H Resonances were assigned based on chemical shifts and ^{13}C,^{1}H-correlation data. The signals of C-atoms bonded to H-atoms were attributed based on HSQC spectra.

The assignment of other C-signals was achieved on the basis of the ^{13}C chemical shifts and long-range HMBC spectra. All chemical shifts are reported in ppm.

The UV spectra of the isolated compounds were recorded with a diode-array detector as the compounds eluted from the HPLC column.

General Procedure for Reactions of Methylglyoxal and Malonaldehyde with Amino Acid Derivatives. The amino acid derivative (N^{α}-acetyllysine: 14.30 mg, 0.076 mmol; *N*-acetylglycyllysine *O*-methyl ester: 14.80 mg, 0.057 mmol; N^{α}-acetylhistidine 19.20 mg, 0.098 mmol) was dissolved in 0.1M phosphate buffer (1 ml) at pH 4.6 and 7.4, resp. Malonaldehyde (hydrolyzed from TMP (40 mg, 0.244 mmol)) was mixed with methylglyoxal (200 µl, 3.306 mmol), and the pH of the mixture was adjusted to 4.6 with 0.1M NaOH. The appropriate aldehyde mixture was then added to the soln. of the amino acid derivative. The reactions were performed at 37°, and the progress of the reactions was monitored by HPLC and LC/MS analyses.

General Procedure for Preparation of Amino Acid Adducts with Methylglyoxal and Malonaldehyde. Malonaldehyde (hydrolyzed from TMP (800 mg, 4.878 mmol)) was dissolved in 10 ml of a 0.1M phosphate buffer at pH 4.6, and 4 ml (66.111 mmol) of methylglyoxal was added. The pH of the mixture was adjusted to 4.6 with 0.1M NaOH. The amino acid derivative (N^{α}-acetyllysine: 290.60 mg, 1.546 mmol; *N*-acetylglycyllysine *O*-methyl ester: 298.40 mg, 1.152 mmol; N^{α}-acetylhistidine 382.50 mg, 1.942 mmol) was dissolved in 20 ml of a 0.1M phosphate buffer (pH 4.6) and was then added to the mixture of the aldehydes. The reactions were performed at 37° for 2 d. Then, the mixtures were concentrated to *ca.* 10 ml and passed through a prep. *C18* column. The column was eluted with H_2O (2 × 100 ml), then with a gradient from 5% to 20% MeCN in H_2O. The fractions containing products were combined, concentrated to *ca.* 10 ml and subjected to further isolation by using a semiprep. *C18* column. For the purification of N^{α}-acetyllysine and of *N*-acetylglycyllysine *O*-methyl ester adducts, the column was eluted isocratically with 0.01M phosphate buffer at pH 7.1 for 3 min and then with a gradient from 0% to 25% MeCN over a course of 17 min at a flow rate of 4 ml/min. The fractions containing the pure compounds were combined, concentrated to *ca.* 10 ml and then desalted by using the same *C18* column. For the purification of N^{α}-acetylhistidine adducts, the column was eluted isocratically with 0.0025M NH_4HCO_3 soln. for 10 min and then with a gradient from 0% to 30% MeCN over the course of 15 min at a flow rate of 4 ml/min.

The solns. containing the pure adducts were combined and evaporated to dryness. The obtained residues were dried by the use of a freeze drying system.

M_1MG-ALys (= N^2-*Acetyl*-N^6-*(2-formyl-1,4-dioxopentan-3-yl)*-L-*lysine*; **1**). Isolated amount 8 mg. UV (LC eluent, 0.01M phosphate buffer, pH 7.1): 265. ^1H- and ^{13}C-NMR spectra: see *Table 1*. ESI-MS (pos.): 315 (100, $[M+H]^+$). MS^2 of 315: 189 (30, $[M+H-$(malonaldehyde-methylglyoxal conjugate unit)$+H]^+$).

M_1MG-Dipep (= *Methyl* N-*Acetylglycyl*-N^6-*(2-formyl-1,4-dioxopentan-3-yl)*-L-*lysinate*; **2**). Isolated amount 9 mg. UV (LC eluent, 0.01M phosphate buffer, pH 7.1): 265. ^1H- and ^{13}C-NMR spectra: see *Table 2*. ESI-MS (pos.): 386 (60, $[M+H]^+$). MS^2 of 386: 260 (100, $[M+H-$(malonaldehyde-methylglyoxal conjugate unit)$+H]^+$).

M_1MG-AHis-a (= N-*Acetyl-1-(2-formyl-1,4-dioxopentan-3-yl)histidine*; **3a**) *and M_1MG-AHis-b* (= N-*Acetyl-3-(2-formyl-1,4-dioxopentan-3-yl)histidine*; **3b**). Isolated amount 30 mg. UV (LC eluent, 0.01M phosphate buffer, pH 7.1): 268. ^1H- and ^{13}C-NMR spectra of the isomer **3a**: see *Table 3*. ESI-MS (pos.): 324 (100, $[M+H]^+$). MS^2 of 324: 198 (75, $[M+H-$(malonaldehyde-methylglyoxal conjugate unit)$+H]^+$).

M_1MG-AHis-b (**3b**). ^1H-NMR (600 MHz, D_2O): 8.81 (*s*, 2 H, CHO); 7.60 (*s*, H–C(2)); 6.82 (*s*, H–C(4)); 4.38 (*dd*, $J = 9.6, 4.6$, H–C(α)); 3.63 (*s*, H–C(b)); 3.07 (*dd*, $J = 13.3, 4.1$, H_a–C(β)); 2.91–2.83 (*m*, H_b–C(β)); 1.94 (*s*, 3 H, acetylhis.); 2.22 (*s*, *Me*C(O)C(b)). ^{13}C-NMR (600 MHz, D_2O): 211.3 (Me*C*(O)C(b)); 192.5 (CHO); 181.1 (COOH); 176.1 (C(O) acetylhis.); 139.9 (C(2)); 132.2 (C(5)); 120.6 (C(4)); 110.2 (C(a)); 58.4 (C(b)); 57.8 (C(α)); 32.4 (C(β)); 28.8 (*Me*C(O)C(b)); 24.9 (Me acetylhis.).

REFERENCES

[1] A. Abordo, H. S. Minhas, P. J. Thornalley, *Biochem. Pharmacol.* **1999**, *58*, 641.
[2] P. J. Thornalley, A. Langbor, H. S. Minhas, *Biochem. J.* **1999**, *344* (Pt1), 109.
[3] M. Kazachkov, P. H. Yu, *J. Chromatogr., B* **2005**, *824*, 116.
[4] G. E. Wuenschell, D. Tamae, A. Cercillieux, R. Yamanaka, C. Yu, J. Termini, *Biochemistry* **2010**, *49*, 1814.
[5] T. Wang, R. Kartika, D. A. Spiegel, *J. Am. Chem. Soc.* **2012**, *134*, 8958.
[6] C. L. Price, S. C. Knight, *Trends Endocrinol. Metab.* **2009**, *20*, 312.
[7] M. Kalousova, T. Zima, V. Tesar, S. Dusilova-Sulkova, J. Skrha, *Mutat. Res.* **2005**, *579*, 37.
[8] L. Lv, X. Shao, H. Chen, C-T. Ho, S. Sang, *Chem. Res. Toxicol*. **2011**, *24*, 579.
[9] B.-H. Lee, W.-H. Hsu, T. Huang, Y.-Y. Chang, Y.-W. Hsu, T.-M. Pan, *J. Agric. Food Chem*. **2013**, *61*, 1288.
[10] M. E. Westwood, P. J. Thornalley, *J. Protein. Chem*. **1995**, *14*, 359.
[11] I. N. Shipanova, M. A. Glomb, R. H. Nagaraj, *Arch. Biochem. Biophys.* **1997**, *344*, 29.
[12] R. H. Nagaraj, I. N. Shipanova, F. M. Faust, *J. Biol. Chem.* **1996**, *271*, 19338.
[13] D. J. Tuma, M. L. Kearley, G. M. Thiele, S. Worrall, A. Haver, L. W. Klassen, M. F. Sorrell, *Chem. Res. Toxicol.* **2001**, *14*, 822.
[14] R. Rolla, D. Vay, E. Mottaran, M. Parodi, N. Traverso, S. Arico, M. Sartori, G. Bellomo, L. W. Klassen, G. M. Thiele, D. J. Tuma, E. Albano, *Hepatology* **2000**, *31*, 878.
[15] D. Pluskota-Karwatka, A. J. Pawłowicz, M. Bruszyńska, A. Greszkiewicz, R. Latajka, L. Kronberg, *Chem. Biodiversity* **2010**, *7*, 959.
[16] D. Pluskota-Karwatka, D. Matysiak, M. Makarewicz, L. Kronberg, *Eur. J. Org. Chem*. **2012**, 4797.
[17] M. O. Lederer, R. G. Klaiber, *Bioorg. Med. Chem*. **1999**, *7*, 2499.
[18] K. Ichihashi, T. Osawa, S. Toyokuni, K. Uchida, *J. Biol. Chem.* **2001**, *276*, 23903.
[19] M. Orioli, G. Aldini, M. C. Benfatto, R. M. Facino, M. Carini, *Anal. Chem*. **2007**, *79*, 9174.
[20] T. Maeshima, K. Honda, M. Chikazawa, T. Shibata, Y. Kawai, M. Akagawa, K. Uchida, *Chem. Res. Toxicol*. **2012**, *25*,1384.
[21] A. Druckova, L. J. Marnett, *Chem. Res. Toxicol*. **2006**, *19*, 1330.
[22] D. Lu, L. A. Peterson, *Chem. Res. Toxicol*. **2010**, *23*, 142.
[23] A. Gómez-Sánchez, I. Hermosin, J.-M. Lassaletta, I. Maya, *Tetrahedron* **1993**, *49*, 1237.
[24] M. Jágr, J. Mráz, I. Linhart, V. Stránský, M. Pospíšil, *Chem. Res. Toxicol.* **2007**, *20*, 1442.
[25] R. Zamora, M. Alaiz, F. J. Hidalgo, *Chem. Res. Toxicol.* **1999**, *12*, 654.
[26] D. Pluskota-Karwatka, A. J. Pawłowicz, L. Kronberg, *Chem. Res. Toxicol.* **2006**, *19*, 921.
[27] D. Steinberg, *J. Biol. Chem*. **1997**, *272*, 20963.
[28] R. B. Bambal, R. P. Hanzlik, *Chem. Res. Toxicol*. **1995**, *8*, 729.
[29] W. M. Valentine, V. Amarnath, K. Amarnath, F. Rimmele, D. G. Graham, *Chem. Res. Toxicol*. **1995**, *8*, 96.
[30] L. I. Szweda, K. Uchida, L. Tsai, E. R. Stadtman, *J. Biol. Chem*. **1993**, *268*, 3342.
[31] K. Stone, M. Ksebati, L. J. Marnett, *Chem. Res. Toxicol*. **1990**, *3*, 33.

Received August 8, 2014